2003 BELTWIDE COTTON CONFERENCES, NASHVILLE, TN – JANUARY 6-10

THE FRITZ-TEXAS A&M DISPERSION MODEL DEVELOPMENT AND COMPARATIVE MODELING WITH ISC3 AND AERMOD

Bradley K. Fritz
USDA-ARS
College Station, TX
Bryan W. Shaw and Calvin B. Parnell, Jr.
Texas A&M University
College Station, TX

Abstract

The air pollution regulatory process involves the permitting of sources of regulated pollutants. Part of the permit process requires sources to demonstrate that the National Ambient Air Quality Standards (NAAQS) are not exceeded as a result of pollutant release. While ambient air sampling may be used to demonstrate compliance with the NAAQS, a source's right to operate is becoming increasingly dependent primarily on dispersion modeling results. Currently used Gaussian based dispersion models do not adequately account for pollutant dispersion resulting from sub-hourly variations in wind speed and direction. This can result in over-estimates of downwind concentration, which may result in costly additional control measures or operating permit being denied. Low elevation releases and close property line boundaries cause low-level agricultural sources, such as cotton gins, to be very sensitive to inappropriate modeling results. This research focused on the issue of developing a methodology to analyze the theoretical degree of dispersion within sub-hourly intervals. The degree of dispersion was based on small time-interval (15 second) meteorological data. Using the results of this analysis a new model that accounts for plume dispersion due to sub-hourly variation in wind speed and direction, was developed. The new model (FTAM) was compared to the currently used regulatory models ISC3 and AERMOD, using concentration predictions downwind of a source typical of a cotton gin. FTAM 24-hour concentrations were generally lower that ISC3 predicted 24-hour concentrations, and similar or slightly higher than AERMOD predicted 24-hour concentrations.

Introduction

The Clean Air Act (CAA) is the predominant piece of legislation providing regulatory guidance in controlling sources of air pollution. These regulatory programs have traditionally fallen into three categories; prohibition of new and existing sources emitting pollution, more stringent controls and permitting requirements for new sources, and addressing specific pollution problems such as hazardous air pollutants and visibility impairment (Brownell, 1999). Relating to all of these categories are the National Ambient Air Quality Standards (NAAQS) which address pollution types and levels associated with public health and welfare.

The ongoing regulatory trend requires sources to demonstrate, either through sufficient sampling or dispersion modeling results that source emissions do not produce off-property concentrations exceeding the NAAQS. Recent efforts to gain an operating permit for a cotton gin resulted in a regulatory preference of modeling results to on-site sampling results. Given that a source's right to operate could primarily hinge on property-line concentration estimates based on modeling, it is essential that the model used is as representative as possible and that the outputs are appropriately applied.

The model approved by EPA and in use by most State Air Pollution Regulatory Agencies (SAPRAS) is Industrial Source Complex (ISC). ISC is applied to small and large sources alike. The same model used to predict downwind concentrations from power plants and other industrial sources is likewise applied to small agricultural sources such as grain elevators, cotton gins, and feed mills. A Gaussian-based model increasingly being used is AERMOD (Atmospheric Dispersion Modeling System). AERMOD was developed as a result of the formation of AERMIC (American Meteorological Society/Environmental Protection Agency Regulatory Model Improvement Committee), whose purpose was to introduce state-of-the-art modeling concepts into the EPA's air quality models. As part of this research, a new model based on science similar to that used in the development of ISC, was developed.

This paper looks at comparing the performance of ISC3, AERMOD, and the newly developed FTAM (Fritz Texas A&M Model) under the same set of input parameters. The initial focus of the paper is on the development of FTAM. Only a brief description of the theory and development of FTAM are presented, as a more detailed report is included in Fritz (2002). Comparative modeling was performed over a period of 10 days using meteorological data collected and resolved into input formats as required for each model

Gaussian-Based Modeling

All Gaussian-based dispersion models assume that at a given distance downwind of a source, the concentration of pollutant, in both the vertical and horizontal directions, can be represented by a normal, or Gaussian, distribution. The degree of plume

spread is controlled by the standard deviations associated with both the horizontal and vertical distributions. The values of the standard deviations are functions of both the downwind distance and variations in meteorological conditions and are represented by the stability parameters σ_y and σ_z.

The Gaussian dispersion equation is the ratio of the emission rate to the wind speed multiplied by the two normal density functions, and is given by Equation 1.

$$C = \frac{Q}{2\pi u \sigma_y \sigma_z} \exp\left(-\frac{1}{2}\frac{y^2}{\sigma_y^2}\right)\left\{\exp\left(-\frac{1}{2}\frac{(z-H)^2}{\sigma_z^2}\right) + \exp\left(-\frac{1}{2}\frac{(z+H)^2}{\sigma_z^2}\right)\right\} \quad (1)$$

where:

C = steady state concentration at a point (x,y,z), $\mu g/m^3$
Q = emission rate, $\mu g/s$
σ_y,σ_z = horizontal and vertical spread parameters, m
u = average wind speed at stack height, m/s
y = horizontal distance from plume centerline, m
z = height of receptor with respect to ground, m
H = effective stack height , m ($H = h+\Delta h$)
h = physical stack height, m
Δh = plume rise, m
(Cooper and Alley, 1986)

A physical representation of this relationship is shown in Figure 1.

The stability parameters, σ_y and σ_z, define the plume spread in the horizontal and vertical directions, respectively. The stability parameter values are a function of the downwind distance from the source and the observed meteorological stability. The most commonly used atmospheric stability classification scheme is that developed by Pasquill and Gifford (Cooper and Alley, 1986). The values of σ_y and σ_z determined using this methodology, typically are referred to as the Pasquill-Gifford (PG) stability parameters. The stability parameter values associated with each stability class were developed from experimental data. Therefore, the values of σ_y and σ_z represent mean observed plume spreads resulting from observed meteorological stability. Additionally, the stability parameter values are a function of the time period over which the experiment occurred, and consequently a function of meteorological variations. This is an important observation. When applying these stability parameters to the Gaussian dispersion equation (Equation 1), the concentration (C) time period is defined. For example, if the stability parameters were based on 15-minute observations, when applied to the Gaussian dispersion equation, the resulting concentration would be a 15-minute concentration.

Despite its simplicity, there is a significant amount of disagreement as to the appropriate time frame in the literature. Beychok (1996) provides a good summation of this matter:

> A major problem with the Gaussian dispersion equation is defining what the calculated concentration C represents when using Pasquill's dispersion coefficients. D.B. Turner states that C represents a 3- to 15-minute average; and American Petroleum Institute dispersion modeling publication believes C represents a 10- to 30-minute average; S.R. Hanna and P.J. Drivas believe C is a 10-minute average; and others attribute averaging times from 5 minutes to 30 minutes. Most agree on a range of 10 minutes to 15 minutes. However, many Environmental Protection Agency computer models used to determine regulatory compliance assume that the Gaussian dispersion equation yields 60-minute average concentrations.

This issue of the most appropriate time frame is the basis of this research. Past work by Zwicke (1998) addresses this problem by applying the Gaussian dispersion equation and stability parameters over short time periods for which meteorological data was recorded. He reported significant improvement in dispersion estimates as compared to ISC. The meteorological data sets used by most SAPRAs for modeling purposes are based on hourly intervals and this does not meet the input data requirements for Zwicke's method. The goal of this research is to develop a new model which appropriately accounts for long periods of meteorological variation while using one-hour averaged meteorological data. The research hypothesis is that new stability parameter values can be determined as a function of the observed meteorological parameter statistics.

Estimation of Plume Spread and the Associated Stability Parameter

Degree of Plume Spread as a Function of Time

The first step toward developing new stability parameters is developing an understanding of the present stability parameters. As stated earlier, there is significant disagreement as to the appropriate application of the PG stability parameters. Therefore, an objective methodology for estimating the plume spread as a function of variations in meteorological parameters is needed. The analysis algorithm developed for this purpose assumes that pollutant spread is predominantly convection driven. In other words, the diffusion of a pollutant as it travels downwind is negligible when compared to its transport by the wind. It was also assumed that the pollutant's travel speed and direction are dictated by instantaneous changes in wind speed and direction.

Meteorological data collected in 15-second interval averages included temperature, relative humidity, barometric pressure, solar radiation, and wind speed and direction. Using the collected data, "parcel" paths were traced as they traveled downwind from some common point of origination (i.e. the source). A "parcel" is merely a unit used to describe some mass of pollutant released during each time interval, with each parcel being equal. Parcels were released at the beginning of each meteorological data interval. For example, at time, t = 0,s, Parcel 1 is released, and at time, t = 15,s, Parcel 2 is released. The travel of each parcel was tracked mathematically based on the average wind speed and direction recorded for each 15-second interval. All parcels originated at the origin (0,0). For each time interval, the distance traveled was determined using wind direction (θ),wind speed (u), and time interval (t=15,s). For each time interval, a parcel's previous (x,y) coordinates were incremented using the calculated displacements ($\Delta x,\Delta y$) (Equations 2 and 3). The parcel trajectories were used to determine the plume spread at different downwind distances. A parcel trajectories plot for a 10-minute period is shown in Figure 2.

$$\Delta x = u \bullet t \bullet \cos\theta \tag{2}$$

$$\Delta y = u \bullet t \bullet \sin\theta \tag{3}$$

The vector averaged wind direction for the entire period was determined. Using the vector average direction and a given downwind distance, a line perpendicular to the average wind direction vector at the given downwind distance was established. The locations of parcel crossings on this line were recorded. The distance from these intersection points and the point where the average wind direction line intersects was determined (Figure 3). These values are denoted as W, and represent a width from plume centerline to a point in the plume where the parcel passed. For a given time period, these W values were fitted to a normal distribution, as shown in Figures 4 and 5. A normal distribution was chosen in order the meet the assumption of normally distribution plume spread inherent in the Gaussian model. The normal distribution fit also allowed for the determination of a standard deviation which corresponds to a stability parameter value. From this fit, the plume spread parameter, σ_y (which will be referred to as σ_{yBKF}), was determined.

We can see from Figure 4, for the example plume trace in Figure 2, at 100 m downwind the normal distribution fitted to the W values. Associated with this normal distribution is a standard deviation (σ) of 18.6 m. Similarly from Figure 5, based on the normal distribution fitted to the W values at 400 m downwind, the associated standard deviation is 64.3 m. This standard deviation along with the downwind distance can be used to estimate the degree of plume spread (θ) using Equation 4. Solving Equation 4 forn θ and substituting in 100 and 18.6, for x and σ (where σ_y equals σ), respectively, our estimated plume spread is about 43.6 degrees. Similarly for x = 400 m and σ =64.3 m, the corresponding degree of plume spread is 38.1 degrees.

$$\sigma_y = \frac{x \bullet \tan\frac{\theta}{2}}{2.15} \tag{4}$$

This methodology was used to develop a FORTRAN code for the purpose of performing similar data reduction for all collected meteorological data. Using this program, each hour of collected meteorological data was analyzed for 2-, 3-, 5-, 10-, 15-, 20-, 30-, and 60-minute intervals, and at 100, 200, 300, 400, 500, 600, 700, 800, 900, and 1000 m downwind. For each interval, the average wind speed and direction, the wind speed and direction standard deviations, solar radiation, and σ_{yBKF}, were determined.

A detailed analysis and comparison of the PG stability parameter, σ_{yPG}, and the calculated stability parameter, σ_{yBKF}, is included in Fritz (2002). In general, the results showed large ranges in the values of σ_{yBKF}, even under similar conditions. Also, agreement of the σ_{yBKF} with σ_{yPG} occurred for time intervals that were less than 60 minutes, but varied as a function of stability classification and downwind distance.

Development of FTAM σ_y – Regression Analysis

The next step was to develop a relationship between the determined 60-minute stability parameter, σ_{yBKF}, and the downwind distance and meteorological parameter statistics. To perform the regression analysis, the parameters significantly affecting

the value of σ_{yBKF} were determined. Based on plots of observed data, it was obvious that the downwind distance affected the value of the predicted stability parameter. It was also observed that as the time interval increased, the value of σ_{yBKF} increased. The major parameter varying as a function of time is wind direction fluctuation. Observed data indicate that the greater the magnitude of change in the wind direction, the greater the spread of the plume, and thus the greater the value of σ_{yBKF}. Also important are the average and standard deviation of the wind speed. Greater wind speeds result in farther transport of a given parcel for a given time interval. The combined effects of wind speed and wind direction significantly affect plume spread. For example, for two hourly periods having the same variation in wind direction, the degree of plume spread will differ if the average wind speeds also differ.

The initial form of the new 60-minute stability parameter, σ_{y60}, was a function of the various parameters along with power and interaction terms. This approach did not result in an acceptable fit, based on R^2 values. Examining the relationships between the various parameters showed that variances in σ_{yBKF} were unequal with varying downwind distance (Figure 6) and wind direction standard deviation (Figure 7). A transformation of σ_{yBKF} was performed in order to counter this problem. Pasquill (1962) suggested the following relationship (Equation 5) between σ_{y60} and wind direction standard deviation (σ_θ).

$$\frac{\sigma_y}{x} \sim \sigma_\theta \tag{5}$$

Pasquill (1962) also presented several plots with the plume width (in degrees) as a function of the standard deviation of wind direction. By solving Equation 4 for theta (θ), Equation 6, which fits the relationship given by Equation 5, is derived.

$$\theta = 2 \bullet \mathrm{ATAN}\ \frac{2.15 \bullet \sigma_y}{x} \tag{6}$$

Figures 8 and 9 are similar to Figures 6 and 7, except that instead of plotting σ_{yBKF} as a function of the standard deviation of wind direction and downwind distance, θ is used. The value of θ was calculated based on the value of σ_{yBKF} and its corresponding downwind distance.

The transformation of σ_{yBKF} to θ (Equation 6), resulted in variances in θ that are much closer to being equal for different standard deviations of wind direction and downwind distances. The next step was to develop the model for the regression fit. Theta (θ) (which along with a designated downwind distance can be used to calculate σ_{y60}) was selected as the dependent variable in the model. The independent variables were downwind distance, average wind speed, standard deviation of wind speed, standard deviation of wind direction, and various polynomial and interaction terms. SPSS was used for the regression analysis. A forward entry method was selected for the analysis. Table 1 shows the resulting change in the R^2 value as predictors were entered by order of significance.

The footnote in Table 1 indicates which predictors were entered into a given model. The following is a key to the variables' names.

- WDSD = Wind direction standard deviation, σ_θ
- WDSDCUB = Wind direction standard deviation cubed, σ_θ^3
- DD = downwind distance (in meters) from the source, x
- WD2WSA = Wind direction standard deviation squared / wind speed averaged interaction, $\sigma_\theta^2 \bullet u$
- WDDDWSL2 = Wind direction standard deviation / downwind distance (in km) from source / wind speed standard deviation interaction,
  $\sigma_\theta \bullet (x/1000) \bullet \sigma_u$
- DDSQRLOW = Square of downwind distance (in m), $(x/1000)^2$
- WSSD = Wind speed standard deviation, σ_u
- WSSDSQR = Square of wind speed standard deviation, σ_u^2
- WSSDCUB = Cube of wind speed standard deviation, σ_u^3
- WSAVGSQR = Square of average wind speed, u^2
- WSSDWDIN = Wind speed standard deviation / wind direction standard deviation interaction, $\sigma_u \bullet \sigma_\theta$
- DDCUBE = Cube of downwind distance (in m), x^3
- WDDDWSLO = Wind direction standard deviation / downwind distance (in km) / wind speed average interaction, $\sigma_\theta \bullet (x/1000) \bullet u$
- WDSDSQR = Square of wind direction standard deviation, σ_θ^2

Based on the results of the regression fit, Table 1, model 9 was chosen. The adjusted R^2 for model 9 is 0.918. Adding parameters into the model did not significantly improve the regression fit. However, all of the above parameters are measured by most meteorological monitoring stations. Therefore, adding any or all of the above parameters (if appropriate) will not add to the monitoring requirements. Note that σ_{y60} is the value of the 60-minute horizontal stability parameter estimated from the regression fit on σ_{yBKF}.

Based on this analysis the best-fit model is as shown in Equation 7.

$$\begin{aligned}\theta = {} & 16.485 + 3.719 \cdot \sigma_\theta - 0.000643 \cdot \sigma_\theta^{\,3} - 0.01904 \cdot \sigma_\theta^{\,2} \\ & - 0.03521 \cdot x + 43.385 \cdot \left(\frac{x}{1000}\right)^2 - 50.323 \cdot \sigma_u + 43.013 \cdot \sigma_u^{\,2} \\ & - 13.293 \cdot \sigma_u^{\,3} + 0.00493 \cdot \sigma_\theta^{\,2} \cdot u - 0.904 \cdot \sigma_\theta \cdot \left(\frac{x}{1000}\right) \cdot \sigma_u\end{aligned} \tag{7}$$

Where all variables are as defined above.

The adjusted R^2 for this model is 0.918. A plot of the predicted value versus the actual value is shown in Figure 10. Figure 11 is a plot of the unstandardized residual versus the unstandardized predicted value.

Comparative Modeling

The next step was to perform side-by-side comparative modeling of FTAM, ISC3 and AERMOD. The appropriate meteorological data inputs for each model were developed using short-term (15-second) meteorological data obtained from a Campbell weather station. As the intent of this comparative modeling was to contrast the 24-hour concentrations predicted from each model for the same pollutant source, the meteorological data was compiled such that each data file represented an entire 24-hour period with one-hour averages for each hourly period. The form and format of these meteorological data files for each model is discussed below.

Meteorological Data Requirements for ISC3, FTAM, and AERMOD

AERMOD required additional parameter calculations in addition to the measured meteorological data. These additional parameters are used by AERMOD to characterize the planetary boundary layer (PBL). The PBL is characterized as either stable (SBL) or convective (CBL). As a steady-state plume model, AERMOD assumes both the vertical and horizontal distributions to be Gaussian in the SBL, and the horizontal to be Gaussian, and the vertical to be bi-Gaussian in the CBL (Cimorelli, 1998).

ISC3 required one meteorological data input file containing hourly averages of meteorological variables, as well as an estimate of stability classification for each hour. The stability classification estimate was based on the Pasquill-Gifford stability classification method and the hourly meteorological data. Likewise, the stability parameters, σ_y and σ_z, were calculated using the Pasquill-Gifford method.

FTAM required one meteorological data file containing hourly averages and standard deviations of meteorological variables. The vertical stability parameter, σ_z, was calculated based on the Pasquill-Gifford method, while the horizontal stability parameter, σ_y, was calculated using the regression fit shown in Equation 7.

Generation of Meteorological Data Files

The meteorological data files used in the comparative modeling analysis were generated from data collected in 15-second intervals. The rough data were separated into individual files, each representing a 24-hour period. The 15-second data were averaged for each hour and the data for each 24 hour period were written to a separate file. This resulted in data files each containing 24, 1-hour data for average solar radiation, average wind direction, average wind speed, wind direction standard deviation, wind speed standard deviation, average temperature, and average barometric pressure. A FORTRAN program was developed to read in the one-hour averaged data files for each 24-hour period, and to use this data to generate the appropriate input files for FTAM, ISC3 and AERMOD.

Sample Source and Receptors

For this comparative modeling analysis a single elevated exhaust source with a height of 6 meters was selected. The diameter of the exhaust pipe was 0.5 meters with an exit velocity of 10 m/s. The emission rate was set at 2.7 g/s PM10. This emission rate corresponds the total emission rate from a gin operating at 18 bales per hour with a PM10 emission factor of 544 g/bale (1.2 pounds per bale)

Receptors were set up as a radial grid. Radial lines were located every 5°, with radial rings every 100 meters out to a distance of 1000 meters. Initial modeling had maximum downwind distances for receptors of 1000 meters. Preliminary results from AERMOD indicated a need for further receptor distances past the 1000 meter distance.

Daily 24-Hour Concentration Predictions

Modeling was performed to predict 24-hour PM-10 concentrations using each of the three models. Ten days of complete meteorological data were available for this analysis.

Table 2 contains the maximum 24-hour concentrations predicted by each model, for each day. Also presented are the downwind distances at which the maximum predicted concentration occurred. Based on Table 2, the average ratios of predicted 24-hour concentrations show that the ISC3 predicted 24-hour concentration was, on average, 130% of the FTAM predicted 24-hour concentration, and 170% of the AERMOD predicted 24-hour concentration. Similarly, the predicted 24-hour concentration from AERMOD was, on average, 80% of the FTAM predicted 24-hour concentration.

A study by Cambridge Environmental Research Consultants (CERC) (2000), the developers of ADMS (Atmospheric Dispersion Modeling System), compares predicted concentrations from ADMS, AERMOD and ISC3. ADMS models atmospheric dispersion using methodologies similar to AERMOD. The CERC study looked at a variety of sources, including short and tall stack rural sources, tall stack urban sources, and area and volume sources. Of interest for this research are the results from the 5- to 10-meter rural short stack sources with flat terrain. This scenario is similar to the source used in the comparative modeling for this research. The study reports ratios for ADMS/AERMOD and ADMS/ISC3. The ratios reported for ADMS/AERMOD are 0.26, 0.34, 0.20, and 0.22. The average ADMS/AERMOD ratio was 0.255. Similarly for ADMS/ISC3, the ratios were 0.15, 0.16, 0.13, and 0.12, which averages to 0.14. The study did not report the ratio between ISC3 and AERMOD, but it can be deduced using relationships in Equations 8, and 9.

$$C_{ADMS} = 0.255 \bullet C_{AERMOD} \quad (8)$$

$$C_{ADMS} = 0.14 \bullet C_{ISC3} \quad (9)$$

These equations mathematically represent the average ratios discussed above. Setting the right-hand-sides of Equations 8 and 9 together and solving for C_{ISC3}, Equation 10 results.

$$C_{ISC3} = 1.82 \bullet C_{AERMOD} \quad (10)$$

For the CERC (2000) study, the predicted 24-hour concentrations from AERMOD for short stack rural sources were, on average, 182% of the predicted 24-hour concentrations from ISC3. Recall that the results presented earlier for this research showed that ISCST3 predicted 24-hour concentrations were, on average, 170% of the AERMOD predicted 24-hour concentrations.

1-Hour Concentration Predictions

A comparison of the predicted 1-hour concentrations was also of interest, as the predicted 24-hour concentrations were merely an average of 24 1-hour concentrations. This comparison used the same source setup. For the 1-hour tests, the receptor grid was changed to a single array of 10 samplers from 100 to 1000 meters (100 meters intervals) along the north axis. The meteorological data used was the same 10 days used for the 24-hour tests, with the exception that all wind directions were changed to north flowing winds. This setup results in concentration predictions at each of the samplers being the maximum 1-hour concentrations. Using the modified meteorological data the 1-hour concentrations for each of the 24 1-hour periods were predicted at each receptor by each model. The 1-hour concentrations were then compared by determining the ratio of C_{ISC3}/C_{FTAM}, C_{AM}/C_{FTAM}, and C_{ISC3}/C_{AM}.

where

C_{FTAM} = FTAM predicted 1-hour concentration
C_{ISC} = ISC3 predicted 1-hour concentration
C_{AM} = AERMOD predicted 1-hour concentration

These ratios were averaged for each downwind distance receptor. Also determined were the minimum and maximum ratios, and 95% confidence intervals. All of these values are presented in Tables 3, 4, and 5.

The most noticeable results from these tables are the wide ranges in the ratios between the model predictions. On average, the ISC3 predicted 1-hour concentration was about 370% of the FTAM predicted 1-hour concentration and (neglecting the 100 meter data) 700% of the AERMOD predicted 1-hour concentration. Also, the AERMOD predicted 1-hour concentration

was 144% of the FTAM predicted 1-hour concentration. Examining the actual 1-hour predicted concentrations, an interesting trend is observed. During the nighttime hours, each of the models tend to predict very low concentrations near the source and the maximum 1-hour concentration farther away from the source. While during the daytime, the maximum predicted 1-hour concentration occurs very near the source. The nighttime behavior is due to the enhanced plume rise which increases downwind displacement of the plume before its downward spread results in a predicted concentration at receptor height.

One major point to be made here is that the FTAM model will not always predict lower 1-hour concentrations than ISC3 (which is basically the Gaussian dispersion equation using the PG stability parameters). In fact, the value of σ_{yBKF} can actually be larger or smaller than σ_{PG}. This means that concentration predictions can also be larger or smaller. What determines the degree of dispersion is meteorological stability.

This comparison of the predicted 1-hour concentrations between FTAM and ISC3 can be extended using information developed in the analysis of the stability parameters. For ISC3, the value of σ_{yPG} is used to predict a 1-hour concentration while for FTAM, the value of σ_{yBKF} is used. For the same source and receptor layout using the same hour of meteorological data, the values of Q, u, σ_z, y, z and H would be identical for both models. This means the difference in the predicted 1-hour concentrations are a result of the applied σ_y. If we assume that the sampler is directly downwind of the source (y = 0), a relationship between C_{ISC3} and C_{BKF} can be determined, as shown in Equation 11. The new term $Ratio_{fy}$ is equivalent to the ratio of the ISC3 predicted 1-hour concentration over the FTAM predicted 1-hour concentration, which is also equal to the ratio of σ_{y60} over σ_{yPG}.

$$\frac{C_{ISC3}}{C_{FTAM}} = Ratio_{fy} = \frac{\sigma_{y60}}{\sigma_{PG}} \tag{11}$$

Tables 6 through 10 contain the data from this analysis for each stability class, downwind distance combination, as well as the low and high ratios for each category, and the overall average of the mean ratios over all distances. The overall average of the mean ratios for all stability classes and downwind distances is 2.6. This means that on average, predicted 1-hour concentration from ISC3 would be 260% of predicted 1-hour concentrations from FTAM. This is similar to the 370% discussed previously. Examining the high and low ratios in Tables 6 through 10, the ISC3 predicted 1-hour concentration could be any where from 32% to 1460% of the FTAM predicted 1-hour concentration. Again, this depends on meteorological stability.

Also interesting are results based on observed trends for the 1-hour concentration predictions during daytime and nighttime hours. A plot of nighttime concentration predictions as a function of downwind distance for each model is shown in Figure 12. Observe that ISC3 and FTAM predict roughly the same concentration while AERMOD predicts lower concentrations up close, and higher concentrations farther out. A plot of the daytime concentration predictions as a function of downwind distance for each model is shown in Figure 13. Observe that AERMOD and FTAM predict roughly the same concentrations, while ISC3 predicts significantly higher concentrations.

Discussion

The initial anticipated outcome of this research was that the new model (FTAM) would result in predicted 1-hour concentrations that were an order of magnitude lower than ISC3 predictions, based on previous work by Zwicke (1998) and Williams (1996). The final results did in fact indicate that there were hours in which the FTAM predicted 1-hour concentrations were as much as 10 to 15 times lower than ISC3 predicted 1-hour concentrations. But on average, FTAM predicted 1-hour concentrations were about 40% of ISC3 predicted 1-hour concentrations. Having had little experience with the use and capabilities of AERMOD, there were no anticipated outcomes; as a consequence the results were very surprising. What was most interesting was that FTAM, while tending to predict 24-hour concentrations that were higher, predicted daytime 1-hour concentrations that were very similar to those made by AERMOD. On the other hand, AERMOD's nighttime predicted 1-hour concentrations tended to be completely different. AERMOD tends to predict the nighttime hours maximum 1-hour concentrations at distances where FTAM and ISC3 predicted the lowest 1-hour concentrations. In terms of dispersion, at night, AERMOD tends to account for less dispersion of the plume than do ISC3 and FTAM. While during daytime hours, both FTAM and AERMOD account for greater plume dispersion than ISC3.

This research only examined the horizontal dispersion characteristics due to limitations in the meteorological monitoring equipment. A 3D sonic anemometer could be used to examine the vertical meteorological variation as well. This would allow for the vertical stability parameter to be analyzed using the methodology developed for the horizontal distribution. If this analysis resulted in findings similar to the horizontal stability parameters results, the predicted concentrations from FTAM could potentially be 40 to 50% lower, in some cases. This would mean that FTAM could likely predict concentrations that are 20% of ISC3. Analysis of the vertical stability may also explain the unexpected differences found in the nighttime dispersion estimates.

It was also anticipated that the new σ_y (σ_{yBKF}) could be estimated as a proportion of σ_{yPG}. This research demonstrated that σ_{yPG} is a step function, whereas the experimental σ_{yBKF} was continuous. The value of σ_{yPG} is dependent upon the stability classification while σ_{yBKF} is dependent upon the observed meteorological statistics. The meteorological data requirement for adopting the σ_{yBKF} methodology meets SAPRA requirements.

Conclusions

This research examined the form and function of the stability parameters associated with Gaussian dispersion modeling. These parameters define the degree of plume spread as a function of the associated variation in meteorological conditions. Examining the traditional Pasquill-Gifford (PG) stability parameters, it was observed that they account for a defined degree of plume spread. It was also observed that this degree of plume spread relates to time only as a function of the variation in meteorological conditions. Based on analysis of small time-interval meteorological data using a parcel trajectory model, there is a significant level of variation in the degree of plume spread within stability class and downwind distance categories. Also observed was that usage of the PG stability parameters accounts only for a single point estimate of plume spread within each category, while the actual plume spread may in fact be greater or less. Using this same parcel trace model a methodology was developed allowing for the degree of plume spread (and thus the associated stability parameter in the horizontal plane) to be estimated using meteorological variation parameters through a regression fit.

This research provides a stepping stone for developing a new model that can be used to provide fair regulation of low-level point sources such as cotton gins, feed mills and grain elevators. This new model uses easily obtained meteorological data consistent with the present format used by most regulatory agencies. At the same time, plume spread resulting from meteorological variation within each hourly period is taken into account. The model purposed here is not put forward as the definitive model but rather as a framework for which site-specific meteorological data can be used to develop a site-representative model.

References

Beychok, M.R. 1996. Air-dispersion modeling and the real world. *Environmental Solutions*. 9(6):24-29.

Brownell, F. W. 1999. Clean Air Act. In *Environmental Law Handbook*. ed. T. F. P. Sullivan, ch. 5, 159-204. Rockville, Maryland: Government Institutes.

Cambridge Environmental Research Consultants. 2000. Comparison of Regulatory Design Concentrations: ADMS versus AERMOD and ISCST3. Available: http://www.cerc.co.uk/epa/index.htm

Cimorelli, A. J., S. G. Perry, A. Venkatram, J. C. Weil, R. J. Paine, et.al. 1998. AERMOD Description of Model Formulation. Version 98314. United States Environmental Protection Agency. Available: http://www.epa.gov/scram001/7thconf/aermod/mfdoc.pdf

Cooper, C. D. and F. C. Alley. 1986. *Air Pollution Control: A Design Approach*. 2nd Edition. Prospect Heights, Illinois: Waveland Press, Inc.

Fritz, B. K. 2002. Dispersion Modeling of Particulate Emissions from Low-Level Point Sources. Ph.D. Dissertation. December 2002. Texas A&M University, College Station, Tx.

Pasquill, F. 1962. *Atmospheric Diffusion: The Dispersion of Windborne Material from Industrial and Other Sources*. London, England: D. Van Nostrand Company.

Turner, D. B. 1994. *Workbook of Atmospheric Dispersion Estimates: An Introduction to Dispersion Modeling*. 2nd Edition. Boca Raton, Florida: CRC Press Inc.

Zwicke, Gregory W. 1998. The Dispersion Modeling of Particulate for Point and Multiple Point Sources in Agriculture. M.S. Thesis. December, 1998. Texas A&M University, College Station, Texas.

Table 1. Model summary statistics of regression fit on theta (θ).

Model	Adj. R^2	Std. Error of the Estimate
1	.782	8.0597
2	.845	6.7815
3	.891	5.6843
4	.897	5.5358
5	.907	5.2656
6	.910	5.1846
7	.910	5.1699
8	.915	5.0176
9	.918	4.9499
10	.918	4.9319
11	.919	4.9158
12	.919	4.9053
13	.919	4.8983
14	.919	4.8941

a Predictors: (Constant), WDSD
b Predictors: (Constant), WDSD, WDSDCUB
c Predictors: (Constant), WDSD, WDSDCUB, DD
d Predictors: (Constant), WDSD, WDSDCUB, DD, WD2WSA
e Predictors: (Constant), WDSD, WDSDCUB, DD, WD2WSA, WDDDWSL2
f Predictors: (Constant), WDSD, WDSDCUB, DD, WD2WSA, WDDDWSL2, DDSQRLOW
g Predictors: (Constant), WDSD, WDSDCUB, DD, WD2WSA, WDDDWSL2, DDSQRLOW, WSSD
h Predictors: (Constant), WDSD, WDSDCUB, DD, WD2WSA, WDDDWSL2, DDSQRLOW, WSSD, WSSDSQR
i Predictors: (Constant), WDSD, WDSDCUB, DD, WD2WSA, WDDDWSL2, DDSQRLOW, WSSD, WSSDSQR, WSSDCUB
j Predictors: (Constant), WDSD, WDSDCUB, DD, WD2WSA, WDDDWSL2, DDSQRLOW, WSSD, WSSDSQR, WSSDCUB, WSAVGSQR
k Predictors: (Constant), WDSD, WDSDCUB, DD, WD2WSA, WDDDWSL2, DDSQRLOW, WSSD, WSSDSQR, WSSDCUB, WSAVGSQR, WSSDWDIN
l Predictors: (Constant), WDSD, WDSDCUB, DD, WD2WSA, WDDDWSL2, DDSQRLOW, WSSD, WSSDSQR, WSSDCUB, WSAVGSQR, WSSDWDIN, DDCUBE
m Predictors: (Constant), WDSD, WDSDCUB, DD, WD2WSA, WDDDWSL2, DDSQRLOW, WSSD, WSSDSQR, WSSDCUB, WSAVGSQR, WSSDWDIN, DDCUBE, WDDDWSLO
n Predictors: (Constant), WDSD, WDSDCUB, DD, WD2WSA, WDDDWSL2, DDSQRLOW, WSSD, WSSDSQR, WSSDCUB, WSAVGSQR, WSSDWDIN, DDCUBE, WDDDWSLO, WDSDSQR
o Dependent Variable: THETA

Table 2. Value and location of predicted maximum 24-hour concentrations of PM-10 from source typical of a cotton gin.

Day	ISC3 Max C_{24} ($\mu g/m^3$)	Downwind Distance (m)	FTAM Max C_{24} ($\mu g/m^3$)	Downwind Distance (m)	AERMOD Max C_{24} ($\mu g/m^3$)	Downwind Distance (m)
1	174	300	155	300	151	800
2	175	100	146	100	121	100
3	430	100	258	100	147	500
4	264	100	182	100	127	100
5	215	100	153	100	103	100
6	230	300	203	200	158	600
7	307	200	235	200	159	100
8	241	200	223	200	234	100
9	285	100	233	100	159	100
10	323	200	271	200	196	100

Table 3. Ratio of 1-hour C_{ISC3} / 1-hour C_{FTAM} – Average, Minimum and Maximum Values.

Downwind Distance (meters)	100	200	300	400	500	600	700	800	900	1000
Average Ratio	3.54	4.11	5.12	5.04	4.64	4.20	3.80	2.37	2.05	1.86
95% Confidence Interval	13.6	61.9	96.2	95.7	84.9	72.9	62.1	20.3	12.1	8.6
Minimum Ratio	0.81	0.71	0.65	0.59	0.55	0.52	0.50	0.48	0.46	0.10
Maximum Ratio	59.3	490.6	762.5	757.7	672.9	577.7	492.5	160.8	95.2	66.7

Table 4. Ratio of 1-hour C_{AM}/1-hour C_{FTAM} – Average, Minimum and Maximum Values.

Downwind Distance (meters)	100	200	300	400	500	600	700	800	900	1000
Average Ratio	2.62	0.63	0.71	0.92	1.15	1.36	1.56	1.71	1.84	1.93
95% Confidence Interval	41.3	6.4	2.9	1.9	1.9	2.0	2.4	2.6	2.9	3.1
Minimum Ratio	0.001	0.0008	0.005	0.03	0.029	0.025	0.023	0.021	0.019	0.017
Maximum Ratio	249.7	50.8	22.9	13.5	9.7	7.98	6.97	5.2	5.56	5.84

Table 5. Ratio of 1-hour C_{ISC3}/1-hour C_{AM} – Average, Minimum and Maximum Values.

Downwind Distance (meters)	100	200	300	400	500	600	700	800	900	1000
Average Ratio	120.9	32.1	6.3	3.9	3.6	3.6	3.6	3.6	3.6	3.7
95% Confidence Interval	325.6	217.1	34.5	11.4	11.7	12.4	12.8	12.9	13.0	13.1
Minimum Ratio	0.103	1.31	0.81	0.65	0.51	0.39	0.32	0.27	0.23	0.21
Maximum Ratio	700.9	944.4	230.2	56.2	69.4	72.4	70.7	67.5	64.0	60.5

Table 6. Ratios of $\sigma_{yBKF}/\sigma_{yPG}$ for Pasquill-Gifford stability class 2.

Downwind Distance (m)	Mean	Minimum	Maximum
100	3.69	0.88	14.41
200	2.63	0.83	7.89
300	2.22	0.80	5.82
400	1.98	0.78	4.78
500	1.84	0.76	4.19
600	1.74	0.71	3.79
700	1.63	0.68	3.42
800	1.54	0.67	3.12
900	1.45	0.65	2.83
1000	1.37	0.61	2.59
Overall Average	**2.01**		

Table 7. Ratios of $\sigma_{yBKF}/\sigma_{yPG}$ for Pasquill-Gifford stability class 3.

Downwind Distance (m)	Mean	Minimum	Maximum
100	2.00	0.71	3.81
200	1.85	0.62	3.50
300	1.74	0.55	3.31
400	1.66	0.49	3.17
500	1.59	0.45	3.07
600	1.53	0.41	2.98
700	1.48	0.39	2.91
800	1.43	0.37	2.83
900	1.39	0.36	2.77
1000	1.36	0.36	2.71
Overall Average	**1.60**		

Table 8. Ratios of $\sigma_{yBKF}/\sigma_{yPG}$ for Pasquill-Gifford stability class 4.

Downwind Distance (m)	Mean	Minimum	Maximum
100	2.35	0.63	10.29
200	1.99	0.52	6.53
300	1.88	0.49	6.44
400	1.77	0.46	5.93
500	1.67	0.43	5.39
600	1.60	0.40	4.96
700	1.54	0.38	4.45
800	1.48	0.35	3.78
900	1.44	0.34	3.61
1000	1.41	0.32	3.43
Overall Average	**1.71**		

Table 9. Ratios of $\sigma_{yBKF}/\sigma_{yPG}$ for Pasquill-Gifford stability class 5.

Downwind Distance (m)	Mean	Minimum	Maximum
100	1.88	1.05	3.70
200	1.78	0.88	3.70
300	1.60	0.78	3.21
400	1.53	0.70	3.17
500	1.48	0.64	3.12
600	1.42	0.59	3.02
700	1.39	0.55	3.02
800	1.36	0.51	2.98
900	1.27	0.46	2.73
1000	1.24	0.44	2.73
Overall Average	**1.50**		

Table 10. Ratios of $\sigma_{yBKF}/\sigma_{yPG}$ for Pasquill-Gifford stability class 6.

Downwind Distance (m)	Mean	Minimum	Maximum
100	6.12	1.46	14.58
200	5.87	1.41	13.96
300	6.95	1.36	12.54
400	6.84	1.32	12.29
500	5.99	1.27	13.31
600	5.61	1.23	11.37
700	5.51	1.18	11.55
800	5.43	1.14	11.46
900	5.97	1.22	11.33
1000	5.89	1.18	11.19
Overall Average	**6.02**		

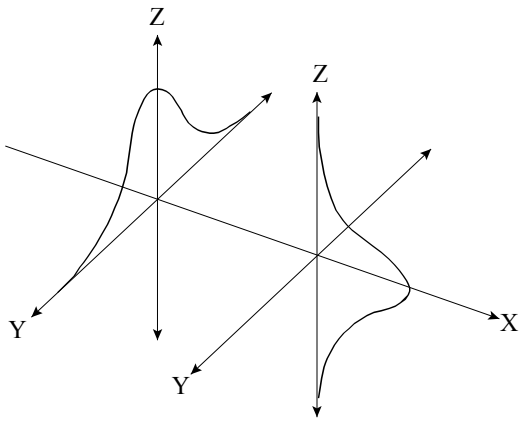

Figure 1. Graphical representation of the Gaussian dispersion model (Turner 1994).

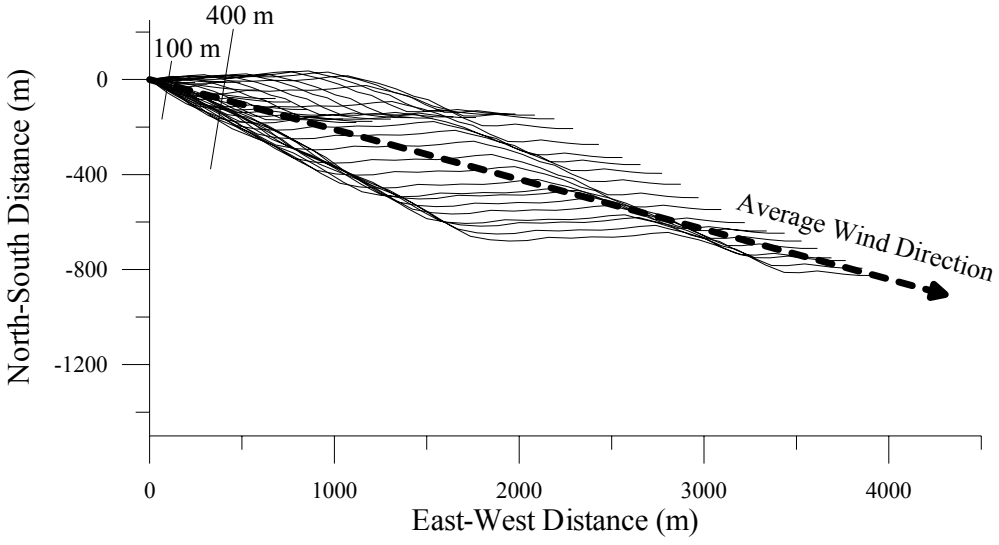

Figure 2. Plot of theoretical 10-minute parcel trace in x-y plane using measured 15-second interval meteorological data.

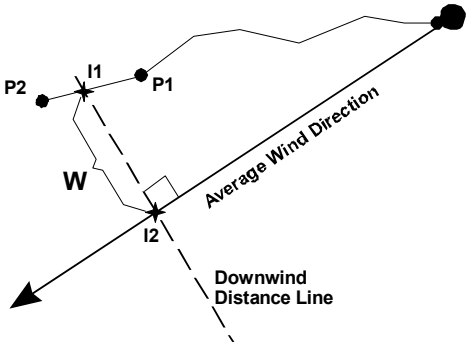

Figure 3. Graphical representation of methodology used to calculate W using theoretical parcel trace data.

where :

P1 and P2 are initial and final (x,y) coordinates of parcels last incremental movements
I1 is the (x,y) coordinates where P1P2 vector intersects Downwind Distance Line
I2 is the (x,y) coordinates where Average Wind Direction line intersects Downwind Distance Line
W is the distance between I1 and I2

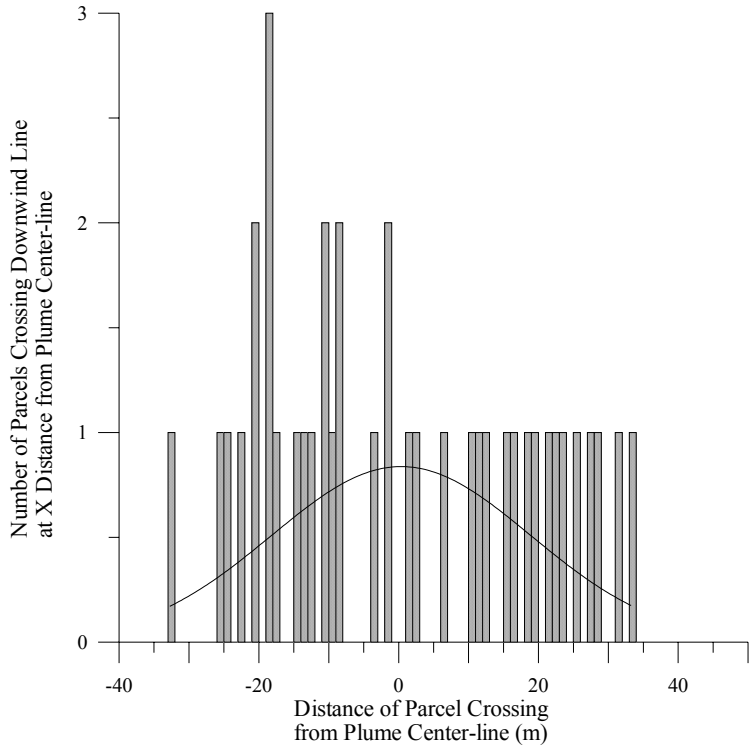

Figure 4. Histogram and normal distribution fit of plume width values, W, as determined from theoretical parcel trace data at 100 m downwind (σ_{yBKF} = 18.6 m).

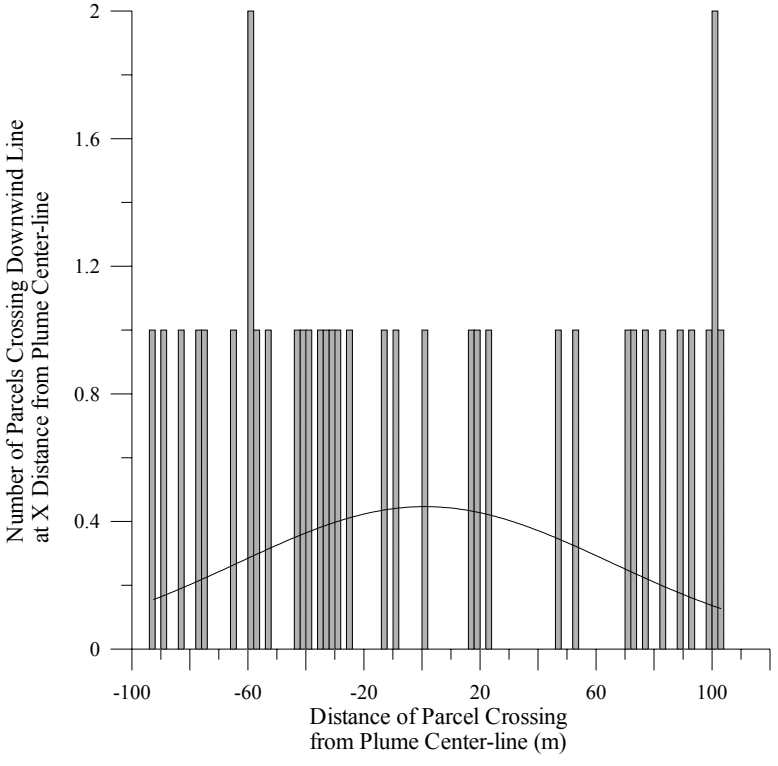

Figure 5. Histogram and normal distribution fit of plume width values, W, as determined from theoretical parcel trace data at 400 m downwind (σ_{yBKF} = 64.32 m).

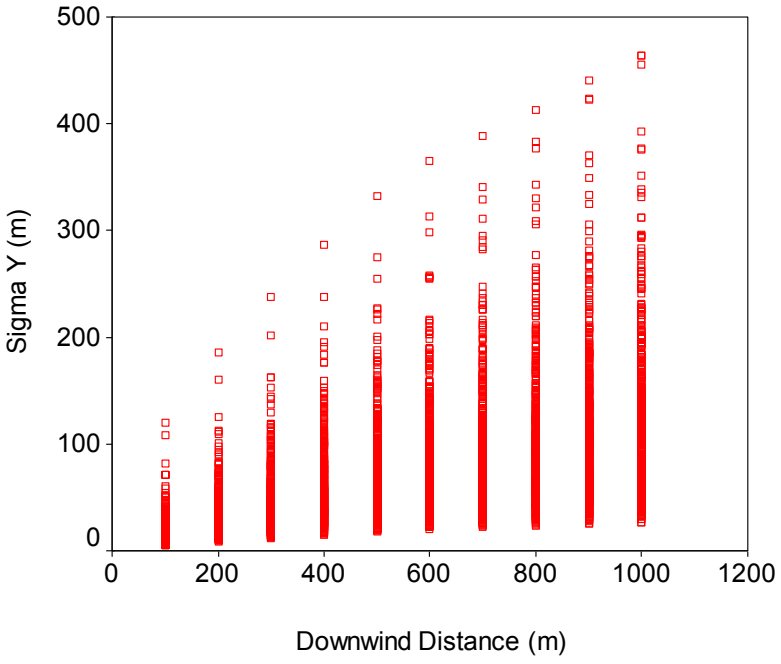

Figure 6. Sigma Y as a function of downwind distance.

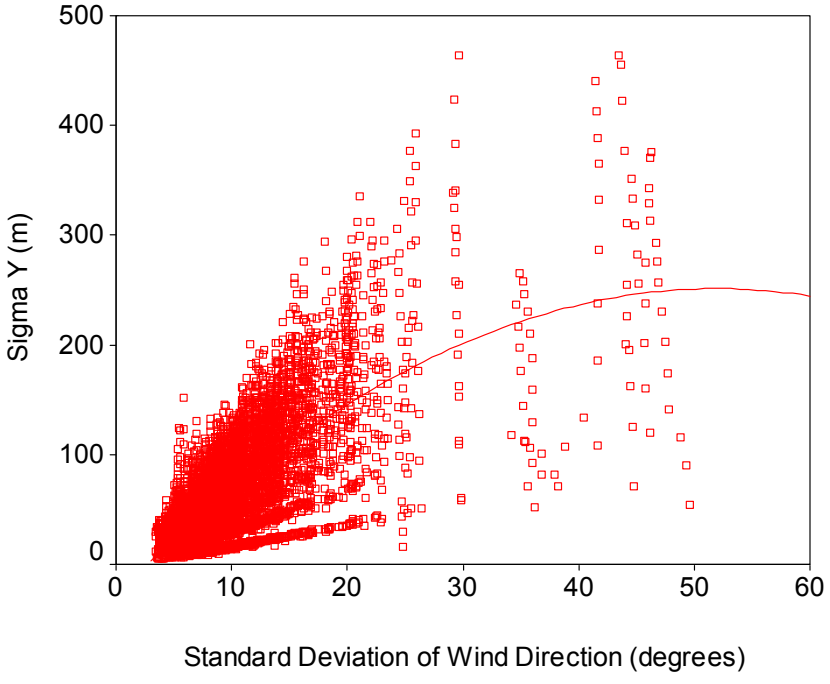

Figure 7. Sigma Y as a function of standard deviation of wind direction ($R^2 = 0.4883$).

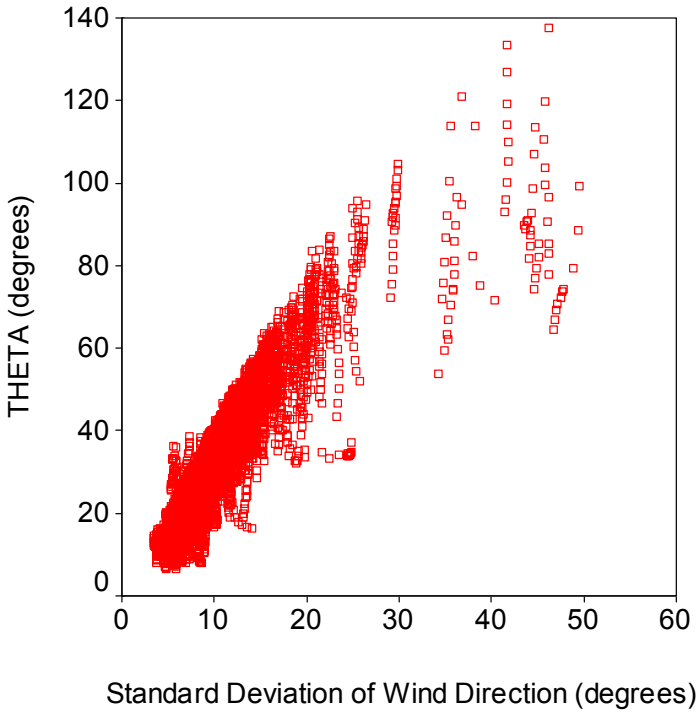

Figure 8. Degree of plume spread (THETA) as a function of standard deviation of wind direction.

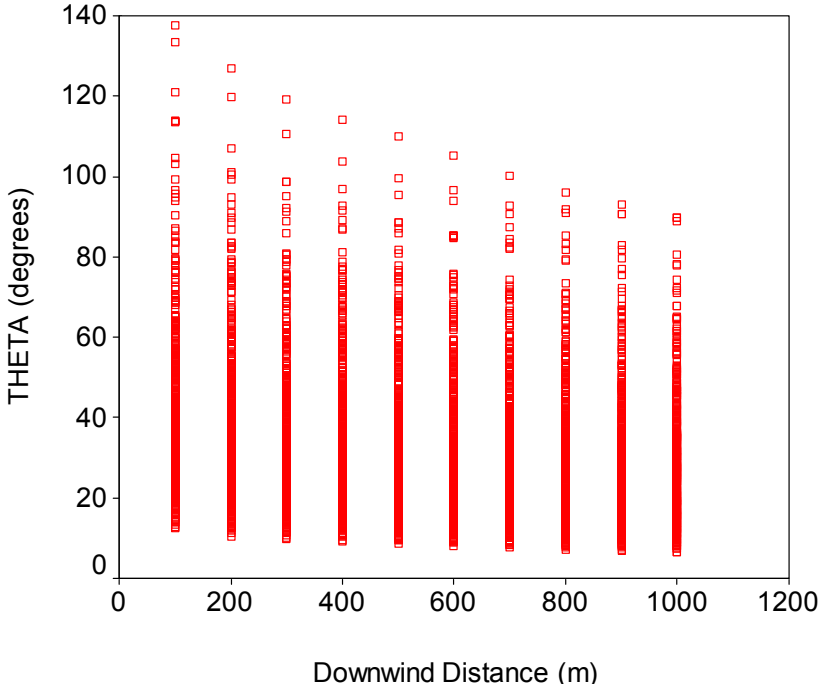

Figure 9. Degree of plume spread (THETA) as a function of downwind distance.

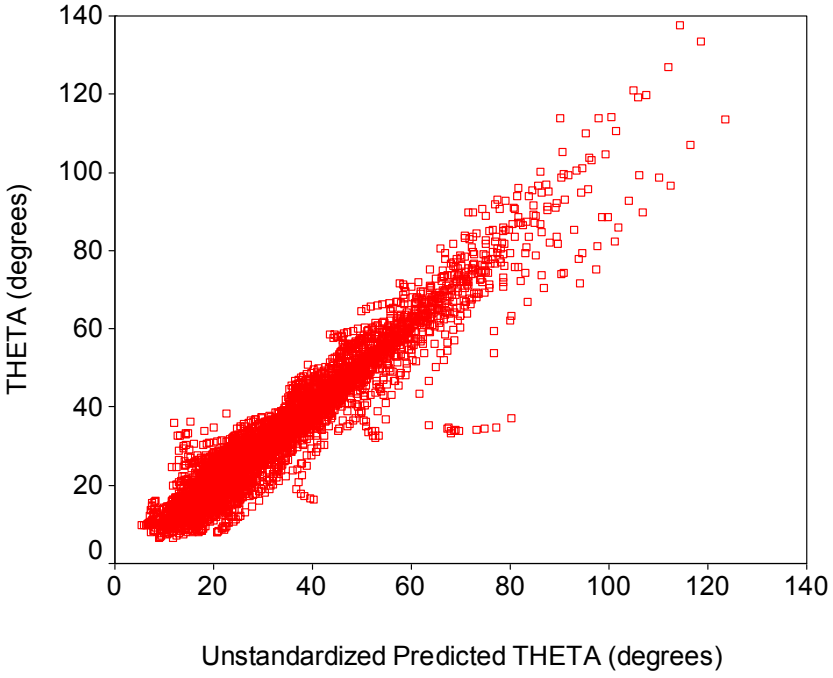

Figure 10. THETA (degrees) versus predicted THETA (degrees).

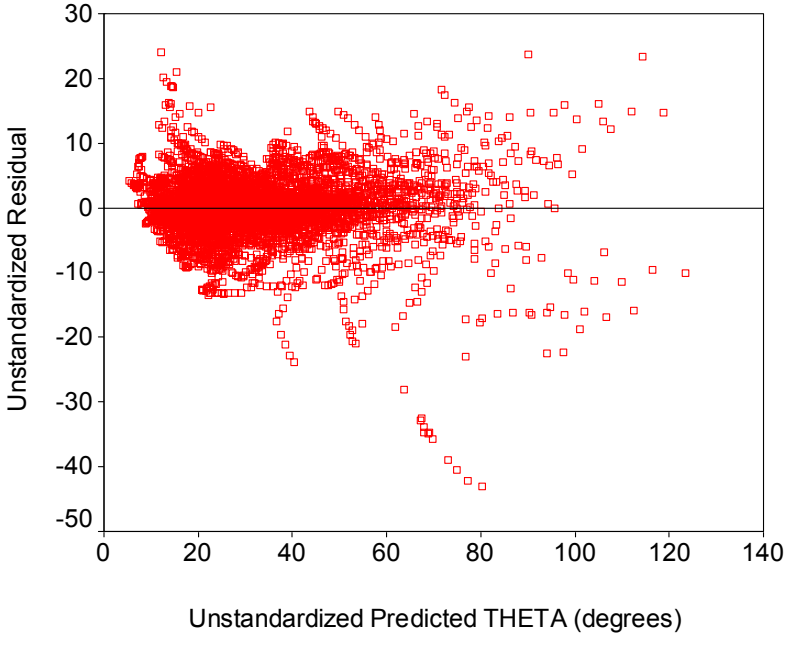

Figure 11. Unstandardized residual versus predicted THETA (degrees).

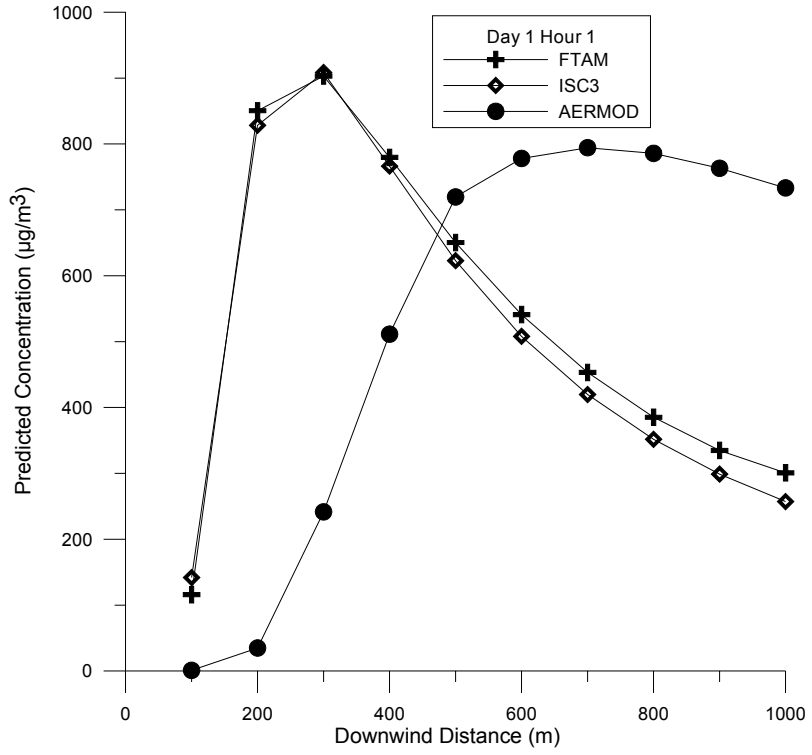

Figure 12. One-hour concentration predictions from ISC3, AERMOD, and FTAM based on an arbitrarily selected hour of meteorological data measured during daytime conditions.

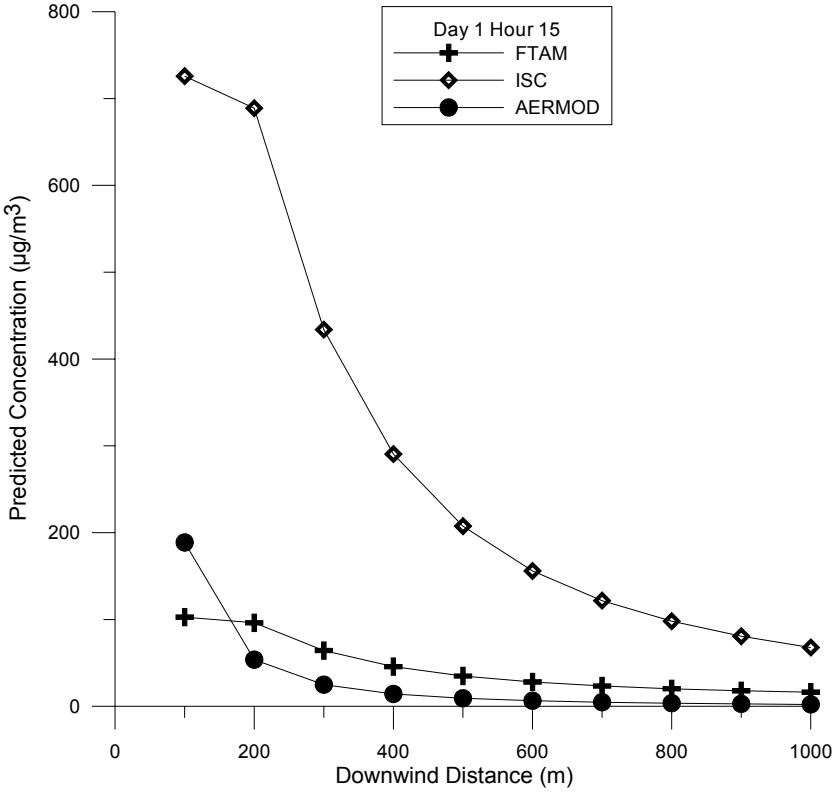

Figure 13. One-hour concentration predictions from ISC3, AERMOD, and FTAM based on an arbitrarily selected hour of meteorological data measured during nighttime conditions.